

Halide Double Perovskite Materials for Stable Lead-Free Perovskite Solar Cells: A Review

Faruk Sani^{a,*} and Suhaidi Shafie^{b,c},

^a Department of Physics, Usmanu Danfodiyo University, 2346, Sokoto, Nigeria.

^b Functional Devices Laboratories, Institute of Advanced Technology, Universiti Putra Malaysia, 43400, Serdang, Malaysia;

^c Faculty of Engineering, Universiti Putra Malaysia, 43400, Serdang, Malaysia;
Corresponding Author: Faruk Sania

Abstract: Lead-based perovskites have shown excellent performance for converting sunlight into electricity. Nevertheless, the toxic nature of lead and instability associated with these promising perovskite light absorbers remained the major issues of concern. This led to immense research effort in finding out alternative materials. Recently, both experimental and computational studies have reported the emergence of halide double perovskite ($A_2BB'X_6$; $X = Cl, Br, I$) as non-toxic and stable materials for lead-free perovskite optical absorbers. The double perovskites compounds attracted attention owing to their interesting properties; thermodynamic stability, appropriate band gap, low excitons binding energy and small carrier effective mass. In this review, thermodynamic stability, electronic properties, various classes of lead-free halide double perovskite, charge carrier transport and effective approaches for the possible substitutions of the divalent lead (Pb^{2+}) cation by a non-toxic pair of monovalent and trivalent cations in halide double perovskites have been discussed. The review also highlights the current research progress on halide double perovskites as well as the future strategy aiming to develop a comprehensive understanding of the photovoltaic behavior of this potential material competing with the lead-based perovskite solar cells.

Keywords: double perovskites, halide, lead-free, solar cells, and stability.

Date of Submission: 16-09-2019

Date of acceptance: 01-10-2019

I. Introduction

Photovoltaic research community has proved the recent perovskite solar cells as the potential runner to compete with silicon solar cells. The first published research on perovskite-based solar cells reported power conversion efficiency (PCE) of ~ 3.0 % in 2009 [1] and recently 22.7 % PCE is confirmed [2]. Perovskite-based light absorbers attracted enormous attention by virtue of their distinctive properties; high absorption co-efficient, tunable band-gap, charges carrier mobility, long diffusion length and inexpensive fabrication methods [3], [4], [5]. Typically there are two major architectural designs of perovskite solar cell; regular (n-i-p) and inverted structure [6], [7]. In regular design, the electron transporting layer is sandwiched between the conductive oxide glass substrate and the perovskite light harvesting layer. In contrast, the inverted design composed of the hole transporting layer deposited just above the conductive oxide coated glass substrate.

Perovskite typically refers to a class of ceramic oxides with the general formula ABX_3 [8], [9]. Where A is organic cation (e.g ammonium, $[NH_4]^+$, hydroxyl-ammonium, $[CH_3OH]^+$, methyl-ammonium, $[CH_3NH_3]^+$, formamidinium, $[CH(NH_2)_2]^+$, ethyl-ammonium, $[CH_3CH_2NH_3]^+$, K^+ and Cs^+ etc) is at the corners of a cube, the X^- anion (commonly halogens: F, Br, Cl, I) is in the middle of each faces and the small B^+ cation is in the middle of the octahedral sites formed by the anions. B is inorganic cation, like group 14 element (e.g Pb^{2+} , Sn^{2+} , Ge^{2+}), alkaline earth metals (such as Mg^{2+} , Ca^{2+} e.t.c), transition divalent metals (such as Cu^{2+} , Zn^{2+} e.t.c), and lanthanide (e.g Eu^{2+} , Yb^{2+}). Each aforementioned B^+ cation could be used as an alternative to replace divalent lead cation (Pb^{2+}) [10]. In a conventional perovskite solar cell ($MAPbI_3$); $[CH_3NH_3]^+$, Pb^{2+} , and I occupied "A", "B" and "X" sites respectively and formed 3D perovskite structure involving a corner sharing of $[BX_6]^-$ octahedral where "A" occupied 12-fold coordinates and counter balanced the charge of BX_3 [11]. ABX_3 structure gives room for modifications in which a range of similar cation or anion with different ionic radius can be substituted [12].

Goldschmidt Tolerance Factor (GTF) expression is usually adopted for the cations and anions match as direct substitution might result in distorted perovskite structure or non perovskite. Goldschmidt Tolerance Factor (GTF) is a dimensionless empirical index which can predict regular crystal structure of a perovskite as shown in equation 1 [12].

$$t = \frac{r_A + r_X}{\sqrt{2}(r_B + r_X)} \quad (1)$$

Where t is the Goldschmidt Tolerance Factor (GTF), r_A represent ionic radius of organic-cation (A), r_B ionic radius of metal- cation (B), and r_X ionic radius of halide- anion (X).

Ideally, GTF, in between 0.9 – 1.0 possesses ideal cubic structure. GTF less than 0.71 or greater than 1.0 result in forming unwanted perovskite structures [13]. When $GTF < 0.8$, indicates that organic cation (A) is very small and this can distort the formation of the perovskite structure, and when $GTF > 1$, the organic cation is very large and this also can result into the formation of non-perovskite. Generally perovskite structure can be obtained in the range, $0.8 \leq GTF \leq 1.0$ [13]. High GTF limit for hybrid iodide perovskites is in the range 1.06 - 1.07 [14]. GTF could not accurately predict ionic radius for hybrid perovskite due to organic cation (A) and hydrogen bond. This complexity is solved by Cheetham and co-workers by applying rigid sphere model for organic cations and assumed rotational freedom and extended the Goldschmidt Tolerance Factor equation to 2 [15].

$$t = \frac{r_{A,eff} + r_X}{\sqrt{2}(r_B + r_X)} \quad (2)$$

$r_{A,eff}$ is given as $r_{mass} + r_{ion}$ Where r_{mass} = the distance from the cation's center of mass to the atom with the largest distance to the center of mass, with the exception of H atoms, r_{ion} = is the corresponding ionic radius [12]. To ascertain the suitability of B- component cation into X_6 , octahedral factor (μ) expression could be applied given in equation 3 resulting in predicting the perovskite stability with $\mu > 0.41$ [14].

$$\mu = \frac{r_B}{r_X} \quad (3)$$

The most efficient divalent metal cation in perovskite-based solar cells is lead (Pb^{2+}) [16]. Lead-based perovskites are one of the major obstacles hindering the implementation and commercialization of this cost effective and efficient solar cells due to toxicity issue of lead [17]. Essentially Pb has no useful role to play in the human bodies, and lead poisoning is responsible for ~ 0.6 % global diseases with the high risk and negative effect on children than adults [18]. To eliminate the toxicity issue in perovskite solar cells, photovoltaic research community published several reports towards achieving a lead-free based perovskite solar cells, and the reports shown significant improvement in extracting and identifying potential candidates to replace for better efficiency and stability [19]. Recently power conversion efficiency (PCE) of 9.0 % was obtained in tin-based perovskite which is the highest PCE reported in lead-free organic-inorganic halide perovskite solar cells [20].

Another approach towards eliminating lead (Pb^{2+}) is by substituting B-site with a pair of heterovalent inorganic cations with +1 and +3 metal cations show a promising direction to solve toxicity issue devolving large scale commercialization. This rises to a new set of perovskite structure with general molecular formula $A_2BB'X_6$ known as Double Perovskite (Elpasolites). The typical structure of the halide double perovskites is indicated in figure 1. Where A could be small cation (e.g Cs or methyl-ammonium), B are metals with +1 charge state (such as Ag, Cu, Au, K, Na, and Tl), B' are elements with +3 charge state (such as Bi, Sb, In, and Ga) and X are halogens (I, Br, Cl) [21], [22], [23], [24]. In this new approach, the regular 3D structure of the perovskite is maintained but the metal cation (Pb^{2+}) at B-site is being substituted by a pair of heterovalent cations with +1 and +3 valence state [21]. The A-site ordered double perovskite $AA'BX_6$ and quadruple perovskite $AA'BB'X_6$ were synthesized but not yet have been found as minerals [25]. [26], used combinatory materials processes and identified fourteen (14) potential double perovskite based on the following requirements; thermodynamic stability, optical absorption, ambipolar carrier conduction and easy carrier, and photon-induced carrier dissociation.

The successful promising candidates are as follows; Cs_2CuSbI_6 , Cs_2CuSBr_6 , $Cs_2CuBiBr_6$, $Cs_2AgBiBr_6$, Cs_2AgSbI_6 , Cs_2AgBiI_6 , $Cs_2AuSbCl_6$, $Cs_2AuBiCl_6$, Cs_2CuSbI_6 , $Cs_2AuBiBr_6$, $Cs_2InSbCl_6$, Cs_2CuSbI_6 , $Cs_2InBiCl_6$, $Cs_2TlSbBr_6$, Cs_2TlSbI_6 , $Cs_2TlBiBr_6$. The author further excluded three Tl-based compounds considering the toxicity of thallium (Tl). Class of compound with $B' = Cu^+$, Ag^+ , and Au^+ (e.g $Cs_2AgBiBr_6$) found to have indirect band gaps and those with direct band gap are have a large optical band gap. This results in poor light absorption and non radiating recombination loss [22].

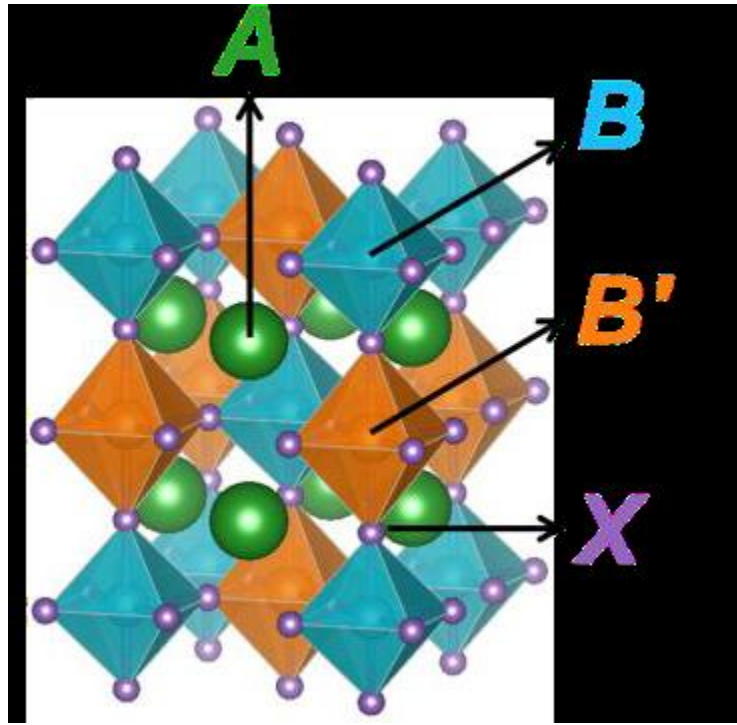


Figure 1. Crystal Structure of Double Perovskite, $A_2BB'X_6$ (A cation is surrounded by BX_6 and $B'X_6$) [27].

II. Phase Stability Of Double Perovskite, $A_2bb'x_6$

Excellent stability of double perovskite upon exposure to the environmental condition has been recently reported [28], [23], [29]. GTF (t) and octahedral factor (μ) are usually the two empirical quantities used to determine structural stability of the double perovskite materials for solar cells application. GTF shows limited accuracy for predicting the stability of certain hybrid halide perovskites [14]. Hence, a new one-dimensional tolerance factor \square has been used that take into consideration both the oxidation states and Shannon ionic radii as expressed in equation 4 [27].

$$\square = \frac{r_X}{r_B} - \eta_A \left(\eta_A - \frac{r_A}{\ln\left(\frac{r_A}{r_B}\right)} \right) \quad (4)$$

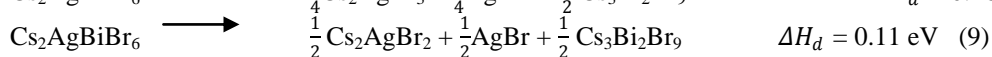
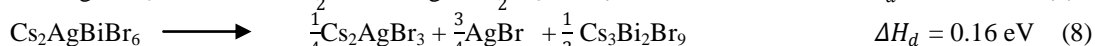
Where η_A is the oxidation state of A.

[27], predicted the stability of several inorganic ($Cs_2BB'Cl_6$) and hybrid organic-inorganic ($MA_2BB'Br_6$) double perovskite compounds significantly better than the commonly Goldschmidt tolerance factor t . The author used data analytic approach based on SISSO (Sure Independence Screening and Sparsifying Operator) and the one dimensional tolerance factor \square .

The long term stability of double perovskite is not yet reported [30]. Hence there is wider room to investigate stable double perovskite to compete with the conventional MAPbI₃ based perovskite. To investigate the chemical stability of the double perovskite material, decomposition enthalpy with respect to possible pathway can be calculated by employing equation 5.

$$\Delta H = 2E[AX] + E[BX] + E[B'X_3] - E[A_2BB'X_6] \quad (5)$$

The above equation interprets the difference between the decomposed binary products and the compound ($A_2BB'X_6$). Moreover, for the stability of $Cs_2AgBiBr_6$, [31] calculated the decomposition enthalpies (ΔH_d) using the following equations:



Further research revealed that Cs_2AgBiI_6 found to be unstable when considering the decomposition in equation 10 with $\Delta H = -0.41 \text{ eV}$ [32].



Similarly, [31] has estimated the decomposition value for Cs_2AgBiI_6 to be -0.47 eV per formula unit through the decomposition pathway in equation 9



The equations 10 and equation 11 above indicate that the $\text{Cs}_2\text{AgBiI}_6$ might be decomposed spontaneously, thus, thermodynamic equilibrium conditions could be hardly satisfied. Incorporation of either I, Cu or Br into one of the identified stable double perovskite could be reduced the band gap and also enhanced the stability. Using this effective approach, [23] has mixed $\text{Cs}_2\text{BiAgCl}_6$ with Cu and resulted structure $\text{Cs}_2\text{BiAg}_{1-x}\text{Cu}_x\text{Cl}_6$ demonstrated remarkable stability. The inconsistency between the experimental and theoretical studies of the thermodynamic stability of $\text{Cs}_2\text{AgBiBr}_6$ proven that the previous first principle calculation of the thermodynamic stability of $\text{Cs}_2\text{AgBiBr}_6$ is incorrect. The commonly used Perdew, Burke, Ernzerhop (PBE) failed to predict the ground state structure of AgBr, AgCl, and CsCl [59].

III. Electronic Properties Of Double Perovskite ($\text{A}_2\text{bb}'\text{x}_6$)

The double perovskites with direct band gap are at higher energy level than those with the indirect band gap [22]. Characteristically, the band gap is the only yardstick for determining the absorption properties of a semiconducting material [23]. By considering an electronic configuration, [26] has classified the double perovskite materials into three main categories: Class-I having an empty s and d outmost orbital (where $\text{B}' = \text{Na}^+, \text{K}^+$ and Rb^+), class-II having an empty s but full d outmost orbital (with $\text{B}' = \text{Cu}^+, \text{Ag}^+$ and Au^+), and class-III possessing full s outmost orbital ($\text{B}' = \text{In}^+$ and Tl^+). The large indirect band gaps exhibited by several double perovskite materials including $\text{Cs}_2\text{AgBiX}_6$ might be due to the chemical mismatch between B and B' heterovalent cations. [32], demonstrated that the combination of Ag^+ and Bi^{3+} results to the large indirect band gaps owing to a mismatch in the atomic orbital. Table 1 shows both calculated and experimental band gaps of several double perovskite materials.

Table 1. Experimental and calculated optical band gaps of double perovskite (direct band gaps are marked with an arrow)

Material	Band gap (eV)	Calculated/Experimental	Reference
$\text{Cs}_2\text{BiCuCl}_6$	2.0	Calculated	[33]
$\text{Cs}_2\text{BiAgCl}_6$	2.7	Calculated	[33]
$\text{Cs}_2\text{BiAuCl}_6$	1.6	Calculated	[33]
$\text{Cs}_2\text{BiCuBr}_6$	1.9	Calculated	[33]
$\text{Cs}_2\text{BiAgBr}_6$	2.3	Calculated	[33]
$\text{Cs}_2\text{BiAuBr}_6$	1.1	Calculated	[33]
$\text{Cs}_2\text{BiCuI}_6$	1.3	Calculated	[33]
$\text{Cs}_2\text{BiAgI}_6$	1.6	Calculated	[33]
$\text{Cs}_2\text{BiAuI}_6$	0.5	Calculated	[33]
$\text{Cs}_2\text{SbCuCl}_6$	2.1	Calculated	[33]
$\text{Cs}_2\text{SbAgCl}_6$	2.6	Calculated	[33]
$\text{Cs}_2\text{SbAuCl}_6$	1.3	Calculated	[33]
$\text{Cs}_2\text{SbCuBr}_6$	1.6	Calculated	[33]
$\text{Cs}_2\text{SbAgBr}_6$	1.9	Calculated	[33]
$\text{Cs}_2\text{SbAuBr}_6$	0.7	Calculated	[33]
$\text{Cs}_2\text{SbCuI}_6$	0.9	Calculated	[33]
$\text{Cs}_2\text{SbAgI}_6$	1.1	Calculated	[33]
$\text{Cs}_2\text{SbAuI}_6$	0.0	Calculated	[33]
$\text{MA}_2\text{AgSbI}_6$	1.93/2.00	Experimental/calculated	[34]
$\text{Cs}_2\text{AgBi}_{0.625}\text{Sb}_{0.735}\text{Br}_6$	1.86	Experimental	[24]
	3.04	Calculated	[35]
$\text{MA}_2\text{KBiCl}_6$			
$\text{Cs}_2\text{InAgCl}_6$	3.3	Experimental	[36]
$\text{Cs}_4\text{CuSb}_2\text{Cl}_{12}$	1.0	Experimental	[37]
$\text{Cs}_2\text{TiI}_2\text{Br}_4$	~ 1.38	Experimental	[38]
$\text{Rb}_2\text{CuInCl}_6$	1.36 [†]	Calculated	[39]
$\text{Rb}_2\text{AgInBr}_6$	1.46 [†]	Calculated	[39]
$\text{Cs}_2\text{AgInBr}_6$	1.50 [†]	Calculated	[39]
$\text{Cs}_2\text{AgInCl}_6$	2.52 [†]	Calculated	[39]
$\text{Rb}_2\text{AgInCl}_6$	2.50 [†]	Calculated	[39]
$\text{Rb}_2\text{AgInBr}_6$	0.63 [†]	Calculated	[39]
$\text{Cs}_2\text{AgBiBr}_6$	1.95	Calculated	[40]

IV. $\text{Cs}_2\text{bb}'\text{x}_6$ Double Perovskite And Its Family

Substitution of a lead (Pb^{2+}) metal cation by a pair of trivalent metal (such as Bi^{3+} , Sb^{3+} , Ga^{3+} , and In^{3+}) and monovalent element (such as Cu^+ , Ag^+ , Au^+) results to a halide double perovskite optical absorber. This type of absorbers maintained the 3D corner sharing octahedral and the neutrality of the cubic structure, which is essential for the appropriate optical band gap and isotropic carrier transport properties [41], [23].

Besides these properties, the double perovskites also demonstrate ferroelectric and ferromagnetic characteristics [42]. Theoretical and experimental reports have revealed that the double perovskite light absorbers exhibit high optical absorbing efficiency in the visible range of the solar spectrum and significant moisture stability in ambient temperature [43]. With respect to the pair combination of B and B', the halide double perovskite could be categorized into four categories: (1) nitrogen family/alkali metals ($B = \text{Bi}^{3+}$ and $B' = \text{Na}^+, \text{K}^+$), (2) nitrogen family/transition metals ($B = \text{Bi}^{3+} \text{Sb}^{3+}$ and $B' = \text{Tl}^+, \text{In}^+$), (3) post transition/noble metals ($B = \text{In}^{3+} \text{Ga}^{3+}$ and $B' = \text{Cu}^+, \text{Ag}^+$), and (4) nitrogen family/noble metals ($B = \text{Bi}^{3+} \text{Sb}^{3+}$ and $B' = \text{Cu}^+, \text{Ag}^+, \text{Au}^+$) [23].

4.0.1 Nitrogen Family/Alkali Metals ($B = \text{Bi}^{3+}$ and $B' = \text{Na}^+, \text{K}^+, \text{Rb}^+$)

The typical example of this compound is $\text{Cs}_2\text{NaBiCl}_6$. This class of materials is not suitable optical absorbers due to relatively large band gap. The large band gap resulted from the anti-bonding state between Bi-*s* and Cl-*p* [26]. Changing the elemental composition in B'-site (from Na^+ to K^+ , to Rb^+) could significantly increase the B'-*s* orbital energy, lifting the conduction band maximum (CBM) and at the same time forming a *p-s* coupling between B and X₆. Thus, resulting in expanding the size of B'X₆ octahedral, contracting BX₆ octahedral and elevating the valence band maximum (VBM) [42]. This indicates that choosing an appropriate element in B'-site and suitable halogen is important in obtaining a desirable band gap.

Pair of nitrogen family (such as Bi^{3+}) and alkali metal (such as K^+) could be used instead of the divalent lead metal with methyl-ammonium iodide (MA) to form the pnictogen/alkali metals double perovskite structure. [35], reported $(\text{MA})_2\text{KBiCl}_6$ in which methyl-ammonium iodide (MA) occupied the A-site cavities to complete the double perovskite structure and maintain the 3D network. The author revealed that band gap of 3.04 eV is obtained from Tauc plot and this is not appropriate for light absorbers in solar cells application. An effort has made to reduce the wider band gap by synthesizing $(\text{MA})_2\text{TlBiBr}_6$ which was found to be isoelectronic with MAPbBr_3 with an optical band gap of ~ 2.0 eV. The obtained band gap is much smaller than the band gap exhibited by $(\text{MA})_2\text{KBiCl}_6$ [44].

4.0.2 Nitrogen Family/Transition Metals ($B = \text{Bi}^{3+} \text{Sb}^{3+}$ and $B' = \text{Tl}^+, \text{In}^+$)

This type of compound, typically, $\text{Cs}_2\text{InBiCl}_6$ have found to show a direct band gap. The band gap characteristics of these materials are quite analogous to APbX₃ based perovskite absorbers due to similar fully occupied outmost *s* orbital of both Bi^{3+} and In^+ [26]. The B'-group plays a vital role in determining the direct band gap or indirect band gap of the double perovskite solar cells. [44] has reported that the band gap is direct when $B' = \text{Tl}^+$, but the band gap is indirect when $B' = \text{Cu}^+$ or Ag^+ due to the large density of 3d states closer to the VBM of the Cu^+ or Ag^+ . The direct band gap could be easily achieved in lead-free halide double perovskite by including an atom with valence *s* states (such as Tl). To verify this, [32] computationally investigated $\text{Cs}_2\text{BiTlBr}_6$ double perovskite where Ag is replaced by Tl and found that *s* state in Tl could be mixed with Bi *s* and anions state, resulting to a direct allowed transition at Γ . The author also noted that the Tl in $\text{Cs}_2\text{BB}'\text{X}_6$ plays a major role in resembling band features of the $\text{Cs}_2\text{Pb}_2\text{Br}_6$ perovskite structure.

On the other hand, toxic nature of Tl counts out compound containing Tl as an alternative candidate to lead-based perovskite. However, the non-toxic $(\text{MA})_2\text{BiInBr}_6$ has not been experimentally reported due to the oxidation of In from +1 to +3 states upon exposure to moisture [23]. However, computational calculations predicted $\text{Cs}_2\text{InBiCl}_6$ and $\text{Cs}_2\text{InSbCl}_6$ as best halide double perovskite absorbers owing to their direct band gap and small effective masses for both electrons (e^-) and holes (h^+) [45]. Further results indicate that the In(I)-based double perovskite are unstable upon exposure to air. An oxidation-reduction reaction is to be considered in predicting the stability of these compounds.

4.0.3 Post Transition/Noble Metals ($B = \text{In}^{3+} \text{Ga}^{3+}$ and $B' = \text{Cu}^+, \text{Ag}^+$)

Recently, double perovskite based on a pair combination of post transition metals ($\text{In}^{3+} \text{Ga}^{3+}$) and noble (Cu^+, Ag^+) have been reported. From first principle calculations, [39] studied the thermodynamic stability and optoelectronic properties of six (6) different post transition/noble metals based double perovskite compounds; $\text{Cs}_2\text{AgInCl}_6$, $\text{Cs}_2\text{AgInBr}_6$, $\text{Rb}_2\text{AgInCl}_6$, $\text{Rb}_2\text{AgInBr}_6$, $\text{Rb}_2\text{CuInCl}_6$, and $\text{Rb}_2\text{AgInBr}_6$ and shown a calculated direct band gaps of 2.52, 1.50, 2.50, 1.46, 1.36 and 0.63 eV respectively. Besides, these compounds exhibit good thermodynamic stability and combination of light electron and heavy hole effective masses. Figure 3 indicates the calculated band gap against the decomposition enthalpy. Post transition (In^{3+})/noble metals (Ag^+) is believed to be a noble direct band gap halide double perovskite with space group $Fm\bar{3}m$. Both the first principle calculations and the experimental reports revealed that $\text{Cs}_2\text{AgInCl}_6$ structure exhibits a direct band gap of 3.3 eV [36]. Furthermore, an empirical analysis on stability of $\text{Cs}_2\text{AgInX}_6$ with respect to their mixed halides based on Goldschmidt tolerance factor (*t*) and octahedral factor (μ) confirm that $\text{Cs}_2\text{InAg}(\text{Cl}_{1-x})_6$ for $x < 1$ is thermodynamically stable [36].

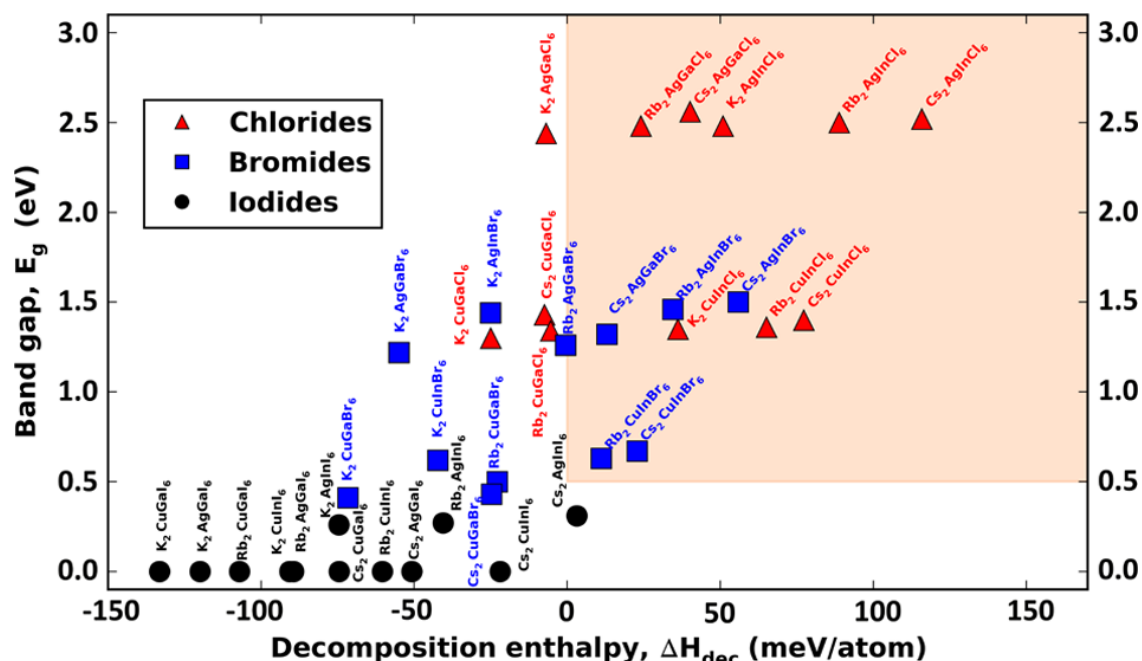


Figure 3. Calculated band gaps plotted against the decomposition enthalpy of all the post transition metals/noble metals halide double perovskite [39]. Reproduced with permission from [39]. Copyright, American Chemical Society, 2017

4.0.4 Nitrogen Family/Noble metals ($B = \text{Bi}^{3+}$, Sb^{3+} and $B' = \text{Cu}^+$, Ag^+ , Au^+)

Majority of the halide double perovskite having indirect band gaps are belong to this category. The indirect band gap associated with the nitrogen family/noble metals could hinder the optimal light absorption efficiency. The typical example of this class is $\text{Cs}_2\text{AgBiCl}_6$. In this material, The indirect band gap is caused by a larger off-centered p - d coupling due to the antibonding hybridized state of $\text{Ag-}d$ and $\text{Cl-}p$ orbitals and it also contributed by the $\text{Bi-}s$ resulting to the mismatch between the $\text{Ag-}d$ and the $\text{Bi-}s$ orbitals [26]. Nevertheless, $\text{Cs}_2\text{AgBiCl}_6$ possesses an interesting property of lone-pair s electron of Bi hoping to imitate the high photovoltaic performance of MAPbI_3 originated from Pb lone-pair s orbital [30]. Noble metals Cu^+ , Ag^+ , Au^+ are usually used in the B' site as monovalent cation due to their good optoelectronic properties [52].

$\text{Cs}_2\text{AgBiCl}_6$ and $\text{Cs}_2\text{AgBiI}_6$ are the first halide double perovskite successfully synthesized using both solid state and solution processable method by [46]. The author reported an indirect band gap of 2.19 eV and 2.77 eV for $\text{Cs}_2\text{AgBiBr}_6$ and $\text{Cs}_2\text{AgBiCl}_6$ respectively. Both compounds have shown remarkable stability upon exposure to air. An optical band gap of stable $(\text{MA})_2\text{AgSbI}_6$ are reported to be 1.93 and 2.00 eV using experimental studies and Density Functional Theory (DFT) calculations respectively [34]. [40] has also reported $\text{Cs}_2\text{AgBiBr}_6$, and the device has shown longer moisture stability compared to $\text{CH}_3\text{NH}_3\text{PbI}_3$. In contrast, [31] examined the thermodynamic stability of $\text{Cs}_2\text{AgBiBr}_6$ using DFT calculations and revealed that the $\text{Cs}_2\text{AgBiBr}_6$ is less stable than the MAPbBr_3 due to weak coupling between $\text{Bi } 6s$ and $\text{Br } 6p$ in the double perovskite $\text{Cs}_2\text{AgBiBr}_6$ unlike the strong $\text{Pb } 6s$ and halogen p coupling in lead-based halide perovskites. Further effort to improve the overall photovoltaic performance of the halide double perovskite is to study their dimensional confinement. [47], synthesized a two-dimensional (2D) double perovskites; $[\text{CH}_3(\text{CH}_2)_3\text{NH}_3]\text{CsAgBiBr}_8$ and $[\text{CH}_3(\text{CH}_2)_3\text{NH}_3]\text{CsAgBiBr}_7$ analogues of the earlier reported three-dimensional (3D) $\text{Cs}_2\text{AgBiBr}_6$ structure. The results indicate that the indirect band gap property of the 3D $\text{Cs}_2\text{AgBiBr}_6$ could be turned to direct band gap in the synthesized layered double perovskites.

Choosing an appropriate synthetic method can easily enhance the stability and increase the optical absorption efficiency of the double perovskites. Nano-crystals of $\text{Cs}_2\text{AgBiI}_6$ was synthesized using an anion exchange reaction by treatment with trimethylsilyl (TMSI). The fabricated device displays strong absorption in the entire visible region and a narrow band gap (~ 1.75 eV) is obtained [48]. Elastic and thermal properties of $\text{Cs}_2\text{AgBiBr}_6$ have examined via density functional theory (DFT) calculations and the results obtained were confirmed by the experimental characterizations. The obtained results indicate that the mechanical and thermal performance of $\text{Cs}_2\text{AgBiBr}_6$ is appreciably better compared to $\text{CH}_3\text{NH}_3\text{PbBr}_3$ based perovskites [43]. Band gap engineering plays a vital role in achieving outstanding photovoltaic (PV) performance within this type of halide perovskites. [24], tailored the band structure of $\text{Cs}_2\text{AgBiBr}_6$ (2.0 eV) via alloying different quantities of Sb/In using DFT with hybrid functional plus spin orbital coupling (HSE+SOC). The calculated indirect band gap is reduced to 1.86eV in $\text{Cs}_2\text{Ag}(\text{Bi}_{0.625}\text{Sb}_{0.25})\text{Br}_6$. This shows that band gap of the double perovskite could be tuned

by changing their chemical compositions. [29], demonstrated the fabrication of $\text{Cs}_2\text{AgBiBr}_6$ via spin coating method and achieved power conversion efficiency (PCE) OF 2.5% as shown in figure 4. The device has proved halide double perovskite as a promising non-toxic and stable material for Pb-free perovskite solar cells. From the studies of the synthesis conditions, the author suggested the necessity of high annealing temperature (about 250°C) for the formation of desired and efficient double perovskite solar cells. For the necessity of high annealing temperature, post annealing and anti-solvent engineering technique were employed in an inverted planar structure solar cell based on $\text{Cs}_2\text{AgBiBr}_6$ and obtained a power conversion efficiency of 2.2 % [53].

Long charge carrier diffusion length > 100 nm was observed in planar structure based on $\text{Cs}_2\text{AgBiBr}_6$ double perovskite solar cells. The results yielded 1% efficiency showing the possibility of the compound in other photovoltaic applications [54]. Good charge transport and extraction has significant effect on photovoltaic performance in solar cells. [55] used transient absorption spectroscopy and studied the photocarrier population in $\text{Cs}_2\text{AgBiBr}_6$ and calculated a life time and steady state carrier density of $1.4 \mu\text{s}$ and $2.2 \times 10^{16} \text{cm}^{-3}$ respectively. The calculated value is greater than the steady carrier density obtained in MAPbI_3 ($5.2 \times 10^{15} \text{cm}^{-3}$). This indicates that $\text{Cs}_2\text{AgBiBr}_6$ has low resistance to charge transport. Similarly, [56] developed a model describing the kinetic process of a photogenerated charge carriers both near the surface and in the bulk of $\text{Cs}_2\text{AgBiBr}_6$ material. The author observed a shallow electron and hole trap state in the bulk of the $\text{Cs}_2\text{AgBiBr}_6$ perovskite. This is an evidenced of mobile charges after under illumination. Another technique was also employed and studied the charge transport in $\text{Cs}_2\text{AgBiBr}_6$ and $\text{Cs}_2\text{AgBi}_{1-x}\text{Sb}_x\text{Br}_6$.

Temperature dependent time resolved microwave conductivity (TRMC) revealed that the dominant scattering process determine the charge transport in halide double perovskite is phonon scattering similar to the one in Pb-based perovskite [60] Nevertheless, double perovskite based solar cells suffered from the effect of hysteresis. To reduce this effect $\text{Cs}_2\text{AgBiBr}_6$ compound, [57] overcome the effect of hysteresis and increase the open circuit voltage in $\text{Cs}_2\text{AgBiBr}_6$ solar cells via interface engineering and material deposition technique. This shows that $\text{Cs}_2\text{AgBiBr}_6$ is a promising alternative light absorber in lead-free perovskite solar cells.

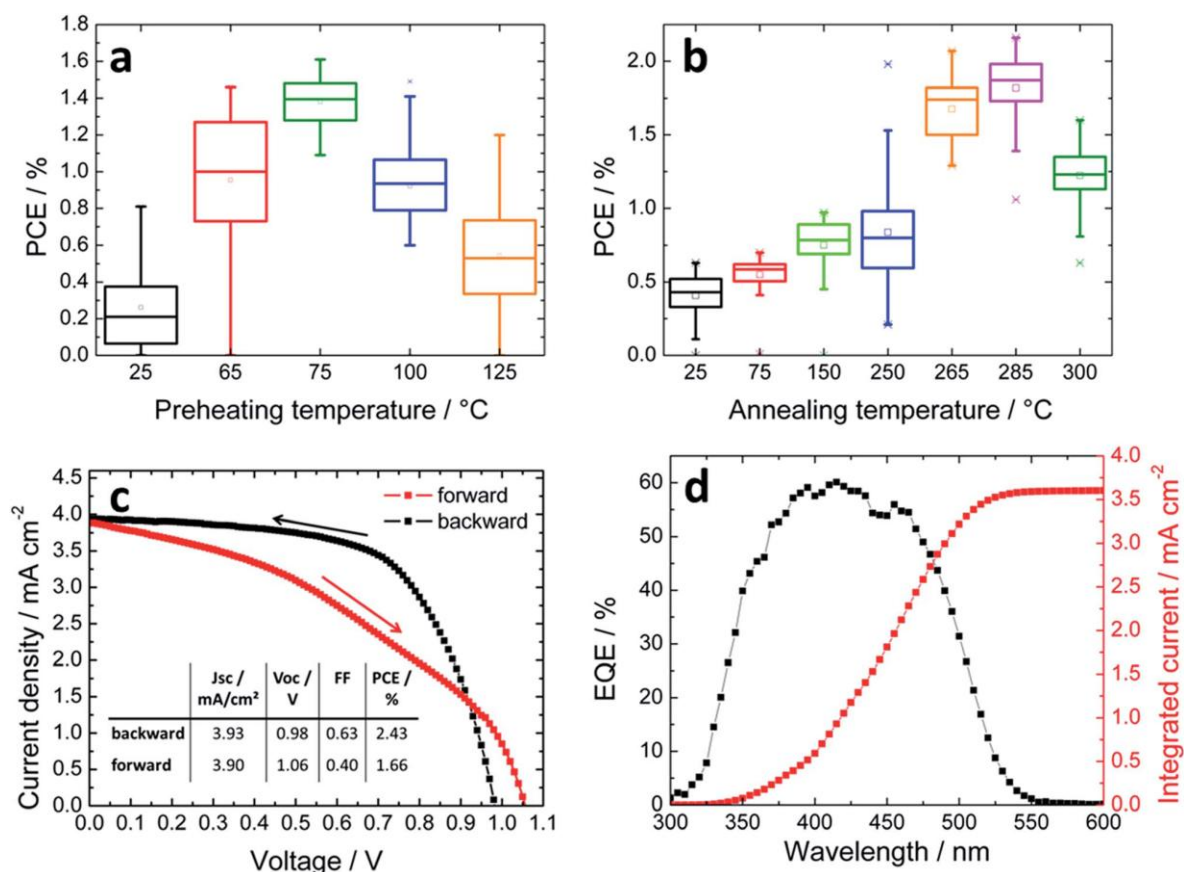


Figure 4. (a) PCE of the device as a function of preheating temperature (b) PCE of the device as a function of annealing temperature (c) J-V characteristic curve of the best performing device and (d) EQE spectrum (black) and integrated predicted current (red) of the device [29]. Reproduced with permission from [29]. Copyright 2017, Royal Society of Chemistry

Very recently, high stability and PCE of 1.37 % were presented using Cs₂AgBiBr₆ double perovskite absorber fabricated in ITO/SnO₂/Cs₂AgBiBr₆/P3HT/Au structure under ambient conditions (temperature; 20-30°C, relative humidity; 40-60 %) [28]. The surface defect of Cs₂AgBiX₆ (X = Cl, Br, I) nanocrystals have recently been studied by [49]. The results prove tunable emission (from 395-575 nm) and sub-band gap trapping (originated from surface defects). The trapping process could be resisted by oleic acid. Doping Cs₂AgBiX₆ (X = Cl, Br, I) with small amount of Pb²⁺ at both B and B'-sites via Density Functional Theory (DFT) has changed the indirect band gap to direct band gap [22]. Solution processing via two-step sequential deposition could be a promising method to synthesize Cs₂AgBiBr₆ [50]. [51], synthesized for the first time MASbSI₂ to prove the possibility of substituting divalent metal cation by +3 and +4 charged cations. Power conversion efficiency of 3.08 % is obtained using MASbSI₂. This study indicates that the chalcogenide can be incorporated into halide perovskite materials for efficient and cost effective perovskite light absorbers.

V. Conclusion

Halide double perovskites have attracted tremendous attention in the photovoltaic community. Both experimental and computational studies were conducted aiming to investigate non-toxic, efficient and stable halide double perovskite light absorbers to replace lead-based perovskites. In the search to a desired trivalent cation, bismuth (Bi³⁺) and antimony (Sb³⁺) have emerged as the best suitable and ruled out arsenic due to its toxic nature. For the monovalent cations, silver (Ag⁺), copper (Cu⁺) and gold (Au⁺) are found to be highly promising due their better electrical conductivity. Among all the reported compounds in this noble class, Cs₂AgBiBr₆ was the only one experimentally fabricated working device and achieved the highest PCE of 2.5 %. Generally, the optoelectronic performance of the halide double perovskites A₂BB'X₆ depends solely on the atomic orbitals and the positions of B and B' cations in the double perovskite structure. It was found that the direct band-gap is obtained when B' is In⁺ or Tl⁺ while the band-gap is indirect when B' is Cu⁺ or Ag⁺. Thus, the electronic structure could be tuned by controlling the lattice sites occupied by the B and B' cations combination. Therefore, to overcome the prevailing challenges associated with the double halide perovskites, B/B' cation combination and configuration required a systematic studies and comprehensive understanding [58]. This can be an effective approach for future research to improve the overall performance of the halide double perovskite solar cells. Furthermore, employing the recent developed modified tolerance factor $\tilde{\alpha}$ would be an accurate method to determine the stability of the halide double perovskites. We hope this review will motivate further experimental synthesis and computational studies to explore high efficient, stable and non-toxic halide double perovskite materials for photovoltaic applications.

Acknowledgments

The work was conducted in Functional Devices Laboratory, Institute of Advanced Technology, Universiti Putra Malaysia. Financial support by Universiti Putra Malaysia, Malaysia via PUTRA grant UPM/800-3/3/1/9629800 is exclusively acknowledged. I am grateful to the collaboration partners, Usmanu Danfodiyo University, Sokoto, Nigeria and Bayero University, Kano, Nigeria.

Author Contributions: Suhaidi Shafie revised the paper and funded the work and Faruk Sani wrote the paper.

Conflicts of Interest: The author declares no conflict of interest.

References

- [1]. A. Kojima, K. Teshima, Y. Shirai, T. Miyasaka, "Organometal Halide Perovskites as Visible- Light Sensitizers for Photovoltaic Cells," *J. Am. Chem. Soc.*, 131 (2009) 6050–6051.
- [2]. "nrel-research-pushes-perovskites-closer-to-market @ www.nrel.gov."(accessed 20 May, 2018) .
- [3]. Q. Chen, N. De Marco, Y. Michael, T. Song, C. Chen, H. Zhao, "Under the spotlight : The organic — inorganic hybrid halide perovskite for optoelectronic applications," *Nano Today*, 10(2015) 355-396.
- [4]. Z. Shi, J. Guo, Y. Chen, Q.Li, Y. Pan, H. Zhang, Y. Xia, W. Huang., "Lead-Free Organic–Inorganic Hybrid Perovskites for Photovoltaic Applications: Recent Advances and Perspectives," *Adv. Mater.*, 29 (2017) 1-28.
- [5]. M. A. Green, A. Ho-Baillie, and H. J. Snaith, "The emergence of perovskite solar cells," *Nat. Photonics*, 8 (2014) 506–514.
- [6]. F. Di Giacomo, A. Fakharuddin, R. Jose, and T. M. Brown, "Progress, challenges and perspectives in flexible perovskite solar cells," *Energy Environ. Sci.*, 9 (2016) 3007–3035.
- [7]. P. Da and G. Zheng, "Tailoring interface of lead-halide perovskite solar cells," *Nano Res.*, 10 (2017) 1471–1497
- [8]. W. Pan, H. Wu, J.Luo, Z. Deng, C.Ge, C. Chen, X. jing, W-J. Yin, G. Niu, L. Zhou *et al.*, "Cs₂AgBiBr₆ single-crystal X-ray detectors with a low detection limit," *Nat. Photonics*, 11 (2017) 726–732.
- [9]. S. F. Hoefler, G. Trimmel, and T. Rath, "Progress on lead-free metal halide perovskites for photovoltaic applications: a review," *Monatshfte fur Chemie*, 148 (2017) 795–826.
- [10]. F. Giustino and H. J. Snaith, "Toward Lead-Free Perovskite Solar Cells," *ACS Energy Lett.*, 1 (2016) 1233–1240.
- [11]. D. T. Gangadharan, Y. Han, A. Dubey, X. Gao, B. Sun, Q. Qiao, R. Izquierdo, D. Ma, "Aromatic Alkylammonium Spacer Cations for Efficient Two-Dimensional Perovskite Solar Cells with Enhanced Moisture and Thermal Stability," *Sol. RRL*, (2018) 1700215.
- [12]. G. P. Nagabhushana, R. Shivaramaiah, and A. Navrotsky, "Direct calorimetric verification of thermodynamic instability of lead halide hybrid perovskites," *Proc. Natl. Acad. Sci.*, 113 (2016) 7717–7721.
- [13]. Z. Li, M. Yang, J. S. Park, S. H. Wei, J. J. Berry, and K. Zhu, "Stabilizing Perovskite Structures by Tuning Tolerance Factor:

- Formation of Formamidinium and Cesium Lead Iodide Solid-State Alloys,” *Chem. Mater.*, 28 (2016) 284–292.
- [14]. W. Travis, E. N. K. Glover, H. Bronstein, D. O. Scanlon, and R. G. Palgrave, “On the application of the tolerance factor to inorganic and hybrid halide perovskites: a revised system,” *Chem. Sci.*, 7 (2016) 4548–4556.
- [15]. G. Kieslich, S. Sun, and A. K. Cheetham, “An extended Tolerance Factor approach for organic–inorganic perovskites,” *Chem. Sci.*, 6 (2015), 3430–3433.
- [16]. A. Babayigit, D.D. Thanh, A. Ethirajan, J. Manca, M. Muller, H-G. Boyen, B. Conings, “Assessing the toxicity of Pb-and Sn-based perovskite solar cells in model organism *Danio rerio*,” *Sci. Rep.*, 6 (2016) 1–11.
- [17]. A. Abate, “Perovskite Solar Cells Go Lead Free,” *Joule*, 1 (2017) 659–664.
- [18]. Childhood Lead Poisoning, <http://www.who.int/ceh/publications/leadguidance.pdf> (retrieved on 20 May 2018).
- [19]. M. Lyu, J. H. Yun, P. Chen, M. Hao, and L. Wang, “Addressing Toxicity of Lead: Progress and Applications of Low-Toxic Metal Halide Perovskites and Their Derivatives,” *Adv. Energy Mater.* 7 (2017) 1602512.
- [20]. S. Shao, J. Liu, G. Portale, H-H. Fang, G.R. Blake, G. Brink, L.A. Koster, M.A. Loi, “Highly Reproducible Sn-Based Hybrid Perovskite Solar Cells with 9% Efficiency,” *Adv. Energy Mater.*, 8 (2018) 1702019.
- [21]. S. Chatterjee and A. J. Pal, “Influence of metal substitution on hybrid halide perovskites: towards lead-free perovskite solar cells,” *J. Mater. Chem. A*, 6 (2018) 3793–3823.
- [22]. J. Kangsabanik, V. Sugathan, A. Yadav, A. Yella, and A. Alam, “Double Perovskites overtaking the single perovskites : A set of new solar harvesting materials with much higher stability and efficiency.,” *phys. Rev. Materials.*, 2 (2016) 1–14, 2016.
- [23]. M. R. Filip, X. Liu, A. Miglio, G. Hautier, and F. Giustino, “Phase Diagrams and Stability of Lead-Free Halide Double Perovskites Cs₂BB'X₆: B = Sb and Bi, B' = Cu, Ag, and Au, and X = Cl, Br, and I,” *J. Phys. Chem. C*, 122 (2018) 158–170.
- [24]. K. Z. Du, W. Meng, X. Wang, Y. Yan, and D. B. Mitzi, “Bandgap Engineering of Lead-Free Double Perovskite Cs₂AgBiBr₆ through Trivalent Metal Alloying,” *Angew. Chemie - Int. Ed.*, 56 (2017) 8158–8162.
- [25]. R. H. Mitchell, M. D. Welch, A. R. Chakhmouradian, and S. Mills, “Nomenclature of the perovskite supergroup: A hierarchical system of classification based on crystal structure and composition,” *Mineral. Mag.*, 81 (2017) 411–461.
- [26]. X. Zhao, X-G. Yang, J-H. Fu, Y. Yang, D. Xu, Q. Yu, L. Wei, S-H. Zhang, “Design of Lead-free Inorganic Halide Perovskites for Solar Cells via Cation-transmutation Design of Lead-free Inorganic Halide Perovskites for Solar Cells via Cation-transmutation,” *J. Am. Chem. Soc.*, 139 (2017) 2630–2638.
- [27]. C. J. Bartel, C. Sutton, B.R. Goldsmith, R. Ouyang, C.B. Musgrave, L.M Ghiringhelli, “New Tolerance Factor to Predict the Stability of Perovskite Oxides and Halides,” arXiv:1801.07700v1 [cond-mat.mtrl-sci], 6 (2018)1–13.
- [28]. C. Wu, C. Zhang, Q. Liu, Y. Luo, W. Guo, X. Huang, Z. Ting, H. Sun, W. Zhong, X. Wei, *et al.*, “The Dawn of Lead-Free Perovskite Solar Cell: Highly Stable Double Perovskite Cs₂AgBiBr₆ Film,” *Adv. Sci.*, 5 (2017) 1700759.
- [29]. E. Greul, M. L. Petrus, A. Binek, P. Docampo, and T. Bein, “Highly stable, phase pure Cs₂AgBiBr₆ double perovskite thin films for optoelectronic applications,” *J. Mater. Chem. A*, 5 (2017) 19972 - 19981.
- [30]. Z. Li and W. Yin, “Recent progress in Pb-free stable inorganic double halide perovskites,” *J. Semicond.*, 39 (2018) 1–6.
- [31]. Z. Xiao, W. Meng, J. Wang, and Y. Yan, “Thermodynamic Stability and Defect Chemistry of Bismuth-Based Lead-Free Double Perovskites,” *Chem. Sus. Chem.*, 9 (2016) 2628–2633.
- [32]. C. N. Savory, A. Walsh, and D. O. Scanlon, “Can Pb-Free Halide Double Perovskites Support High-Efficiency Solar Cells?,” *ACS Energy Lett.*, 1 (2016) 949–955.
- [33]. G. Volonakis, M.R. Filip, A.A. Haghighirad, N. Sakai, B. Wenger, H.J. Snaith, F. Giustino, “Lead-Free Halide Double Perovskites via Heterovalent Substitution of Noble Metals,” *J. Phys. Chem. Lett.*, 7 (2016) 1254–1259.
- [34]. Y.-J. Li, T. Wu, L. Sun, R-X. Yang, L. Jiang, P-F. Cheng, Q-Q. Hao, T-J. Wang, R-F. Lu, W.Q. Deng, “Lead-free and stable antimony–silver-halide double perovskite (CH₃NH₃)₂AgSbI₆,” *RSC Adv.*, 7 (2017) 35175–35180.
- [35]. F. Wei, Z. Deng, S. Sun, F. Zhang, D.M. Evans, G. Kieslich, S. Tominaca, M.A. Carpenter, J. Zhang, P.D. Bristowe, A.K. Cheetham, “Synthesis and Properties of a Lead-Free Hybrid Double Perovskite: (CH₃NH₃)₂AgBiBr₆,” *Chem. Mater.*, 29 (2017) 1089–1094.
- [36]. G. Volonakis, A.A. Haghighirad, R.L. Milot, W.H. Sio, M.R. Filip, B. Wenger, M.B. Johnston, L.M. Herz, H.J. Snaith, F. Giustino, “Cs₂InAgCl₆: A New Lead-Free Halide Double Perovskite with Direct Band Gap,” *J. Phys. Chem. Lett.*, 8 (2017) 772–778.
- [37]. B. Vargas, E. Ramos, E. Pérez-Gutiérrez, J. C. Alonso, and D. Solis-Ibarra, “A Direct Bandgap Copper-Antimony Halide Perovskite,” *J. Am. Chem. Soc.*, 139 (2017) 9116–9119.
- [38]. M. G. Ju, M. Chen, Y. Zhou, H-F, Garces, J. Dai, L. Ma, N.P. Padture, X.C. Zheng, “Earth-Abundant Nontoxic Titanium(IV)-based Vacancy-Ordered Double Perovskite Halides with Tunable 1.0 to 1.8 eV Bandgaps for Photovoltaic Applications,” *ACS Energy Lett.*, 3 (2018) 297–304.
- [39]. X. G. Zhao, D. Yang, Y. Sun, T. Li, L. Zhang, L. Yu, A. Zunger, “Cu-In Halide Perovskite Solar Absorbers,” *J. Am. Chem. Soc.*, 139 (2017) 6718–6725.
- [40]. A. H. Slavney, T. Hu, A. M. Lindenberg, and H. I. Karunadasa, “A Bismuth-Halide Double Perovskite with Long Carrier Recombination Lifetime for Photovoltaic Applications,” *J. Am. Chem. Soc.*, 138 (2016) 2138–2141.
- [41]. L. Debbichi, S. Lee, H. Cho, A.M. Rappe, K-H. Hong, M.S. Jang, H. Kim, “Mixed Valence Perovskite Cs₂Au₂I₆: A Potential Material for Thin-Film Pb-Free Photovoltaic Cells with Ultrahigh Efficiency,” *Adv. Mater.*, 30 (2018) 1–6
- [42]. Q. Zhang, F. Hao, J. Li, Y. Zhou, Y. Wei, and H. Lin, “Perovskite solar cells : must lead be replaced – and can it be done?,” *Sci. Technol. Adv. Mater.*, 6996 (2018) 1–37.
- [43]. L. Dong, S. Sun, Z. Deng, W. Li, F. Wei, Y. Qi, Y. Li, X. Li, P. Lu, U. Ramamurty, “Elastic properties and thermal expansion of lead-free halide double perovskite Cs₂AgBiBr₆,” *Comput. Mater. Sci.*, vol. 141 (2018) 49–58.
- [44]. Z. Deng, F. Wei, S. Sun, G. Kieslich, A. K. Cheetham, and P. D. Bristowe, “Exploring the properties of lead-free hybrid double perovskites using a combined computational-experimental approach,” *J. Mater. Chem. A*, 4 (2016) 12025–12029.
- [45]. Z. Xiao, K. Z. Du, W. Meng, J. Wang, D. B. Mitzi, and Y. Yan, “Intrinsic Instability of Cs₂In(I)M(III)X₆(M = Bi, Sb; X = Halogen) Double Perovskites: A Combined Density Functional Theory and Experimental Study,” *J. Am. Chem. Soc.*, 139 (2017) 6054–6057.
- [46]. E. T. McClure, M. R. Ball, W. Windl, and P. M. Woodward, “Cs₂AgBiX₆(X = Br, Cl): New Visible Light Absorbing, Lead-Free Halide Perovskite Semiconductors,” *Chem. Mater.*, 28 (2016) 1348–1354.
- [47]. B. A. Connor, L. Leppert, M. D. Smith, J. B. Neaton, and H. I. Karunadasa, “Layered Halide Double Perovskites: Dimensional Reduction of Cs₂AgBiBr₆,” *J. Am. Chem. Soc.*, 140 (2018) 5235 - 5240.
- [48]. S. E. Creutz, E. N. Crites, M. C. De Siena, and D. R. Gamelin, “Colloidal Nanocrystals of Lead-Free Double-Perovskite (Elpasolite)

- Semiconductors: Synthesis and Anion Exchange to Access New Materials,” *Nano Lett.*, 18 (2018) 1118–1123.
- [49]. K. Han, J. Chen, S. Yang, F. Hong, L. Sun, P. Han, T. Pullerits, W. Deng, K. Han, “Lead-Free Silver-Bismuth Halide Double Perovskite Nanocrystals,” *Angew. Chemie Int. Ed.*, 130 (2018) 5457 - 5461.
- [50]. M. Pantaler, C. Fettkenhauer, L. Nguyen, A.I. Hoang, C.L. Doru, “Deposition routes of Cs₂AgBiBr₆ double perovskite for photovoltaic application,” *MRS Adv.* (2018) DOI: 10.1557/adv.2018.151
- [51]. R. Nie, A. Mehta, B. W. Park, H. W. Kwon, J. Im, and S. Il Seok, “Mixed Sulfur and Iodide-Based Lead-Free Perovskite Solar Cells,” *J. Am. Chem. Soc.*, 140 (2018) 872–875.
- [52]. E. Meyer, D. Mutukwa, N. Zingwe, and R. Taziwa, “Lead-Free Halide Perovskites: A Review of the Structural, Optical, and Stability Properties as Well as Their Viability to Replace Lead Halide Perovskites” *Metals*, 8 (2018) 667 DOI: 10.3390/met8090667.
- [53]. W. Gao, C. Ran, J. Xi, B. Jiao, W. Zhang, M. Wu, X. Hou, and Z. Wu, “High Quality Cs₂AgBiBr₆ Double Perovskite Film for Lead-Free Inverted Planar Heterojunction Solar Cells with 2.2 % Efficiency” *ChemPhyChem*, 2018, 10.1002.cphc.201800346.
- [54]. W. Ning, F. Wang, B. Wu, J. Lu, Z. Yan, X. Liu, J-M. Liu, W. Huang, M. Fahlman, L. Hultman, T.C. Sum, and F. Gao, “Long Electron-Hole Diffusion Length in High Quality Lead-Free Double Perovskite Film, *Adv. Mater.* 30 (2018) 1706246.
- [55]. R.L.Z. Hoye, L. Eyre, F. Wei, F. Brivio, A. Sadhanala, S. Sun, W. Li, K.H.L. Zhang, J.L. MacManus-Driscoll, P.D. Bristowe, R.H. Friend, A.K. Cheetham, and F. Deschler, “Fundamental Carrier Lifetime Exceeding 1 μm in Cs₂AgBiBr₆ Double Perovskite. *Adv. Mater. Interfaces*, 2018, 1800464.
- [56]. D. Bartesaghi, A.H. Slavney, M.C. Gelvez-Rueda, B.A. Connor, F.C. Grozema, H.A. Karunadasa, and T.J. Sevenje, “Charge Carrier Dynamics in Cs₂AgBiBr₆ Double Perovskite. *J. phys.Chem. C*, 2018, 122, 4809-4816, doi: 10.1021/acs.jpcc.8b00572
- [57]. W. Pantalar, K.T. Cho, V. Quelo, I.G. Benito, C. Fettkenhauer, I. Anusca, M.K. Nazeeruddin, D.C. Lupascu, and G. Grancini, “Hysteresis-Free Lead-Free Double Perovskite Solar Cells by Interface Engineering” *ACS Energy*, 2018.
- [58]. P. Zhang, J. Yang, and S.H. Wei, “Manipulation of Cation Combination of Halide Double Perovskites for Solar Cells Absorbers” *J. Mater. Chem. A*, 2017, DOI: 10.1039/C7TA09713A.
- [59]. D. Han, T. Zhang, M. Huang, D. Sun, M-H. Du, and S. Chen, “Predicting the Thermodynamic Stability of Double Halide Perovskite Halides from Density Functional Theory”. *APL Materials*, 2018, 6, 084902.
- [60]. E.M. Hutter, D. Bartesaghi, M.C. Gelvez-Rueda, and F.C. Grozema, “Band-Like Charge Transport in Cs₂AgBiBr₆ and Mixed Antimony-Bismuth Cs₂AgBi_{1-x}Sb_xBr₆ Halide Double Perovskite” *ACS Omega*, 2018, 3, 11655-11662, DOI: 10.1021/acsomega.8b01705.

Faruk Sania " Halide Double Perovskite Materials for Stable Lead-Free Perovskite Solar Cells: A Review" *IOSR Journal of Electrical and Electronics Engineering (IOSR-JEEE)* 14.5 (2019): 51-60.